JOURNAL OF CATALYSIS 91, 272–282 (1985)

Metal Segregation in Supported Bimetallic Catalysts: γ-Al_2O_3-Supported CO Hydrogenation Catalysts Prepared from $RhOs_3$, Rh_4, and $FeOs_3$ Clusters

J. R. BUDGE,*[1] B. F. LÜCKE,*[2] B. C. GATES,*[3] AND J. TORAN†

*Center for Catalytic Science and Technology, Department of Chemical Engineering, University of Delaware, Newark, Delaware 19716 and †Experimental Station, E. I. DuPont de Nemours and Company, Wilmington, Delaware 19898

Received April 2, 1984; revised September 15, 1984

Al_2O_3-supported metals were prepared from $[H_2RhOs_3(CO)_{10}$(acetylacetonate)], $[Rh_4(CO)_{12}]$, and $[H_2FeOs_3(CO)_{13}]$. The samples were characterized by infrared spectroscopy after reaction with CO + H_2 and tested as catalysts for conversion of CO + H_2 in a flow reactor at 200 and 270°C and 10 atm. Used catalysts were characterized by transmission electron microscopy, X-ray photoelectron spectroscopy, infrared spectroscopy, and elemental analysis. The catalyst lost Os during operation, presumably as a result of formation of volatile carbonyls. The catalytic reaction products were a nearly Schulz–Flory–Anderson distribution of hydrocarbons with small yields of dimethyl ether (formed from methanol). The performance of the catalyst prepared from the $RhOs_3$ cluster was closely similar to that of the catalyst prepared from the Rh_4 cluster. Characterization of the samples after treatment in CO + H_2 and after catalysis demonstrated that the $RhOs_3$ clusters broke apart, first giving triosmium clusters and mononuclear Rh complexes and then, at higher temperatures, giving Rh crystallites and mononuclear Os complexes. The catalytic activity for hydrocarbon synthesis is attributed to the Rh metal; the activity for methanol synthesis is tentatively associated with ionic Rh complexes. The $FeOs_3$ catalyst was two orders of magnitude less active than the Rh Os_3 catalyst, apparently consisting of small iron oxide particles and mononuclear Os complexes. The selectivity of this catalyst for dimethyl ether formation increased markedly with time on-stream in the flow reactor; after 55 h, 36 mol% of the organic product was ether.

INTRODUCTION

Supported bimetallic catalysts are becoming increasingly important as new combinations of metals and supports are found to offer opportunities for control of catalytic activity, especially when the metals are used in high dispersions (*1*). Much remains to be learned about the structures of these catalysts, since it is difficult to obtain good characterizations of very small metal species. Our approach was to begin with structurally simple supported metals having well-defined compositions—molecular metal clusters—and to investigate the evolution in structure and its relation to performance in catalytic hydrogenation of CO—a structure-sensitive probe reaction providing a range of selectivity data.

Most of the experiments were done with γ-Al_2O_3-supported catalysts prepared from $[H_2RhOs_3(CO)_{10}(acac)]$ (where acac is acetylacetonate), a cluster chosen to have one metal (Rh) with a relatively high activity and the other (Os) with a relatively low activity; the Rh is also of interest because it exhibits various selectivities depending on the dispersion, the nature of the support, and possibly the metal oxidation state (*2*). Complementary experiments were done

[1] Present address: The Standard Oil Company, Cleveland, Ohio 44128.

[2] Present address: Zentralinstitut für Organische Chemie, Akademie der Wissenschaften der DDR, Berlin.

[3] To whom correspondence should be addressed.

0021-9517/85 $3.00

with the monometallic catalyst prepared from $[Rh_4(CO)_{12}]$, and a few were done with catalysts prepared from a second bimetallic cluster, $[H_2FeOs_3(CO)_{13}]$. Experiments were also done with catalysts prepared from $[H_2RuOs_3(CO)_{13}]$ and $[H_4Ru_4(CO)_{12}]$, the results being reported separately (*3*).

EXPERIMENTAL

Catalyst Preparation

The metal clusters $[H_2RhOs_3(CO)_{10}(acac)]$ (*4*), and $[H_2FeOs_3(CO)_{13}]$ (*5*) were prepared by methods described in the literature; $[Rh_4(CO)_{12}]$ was purchased from Strem.

The γ-Al_2O_3 support was Catapal SB, obtained in extrudate form from Conoco (Batch No. 8902L). It had a surface area of 274 m^2/g and a pore volume of 0.80 cm^3/g. The support was ground and sieved; the 40–80 mesh fraction was used for catalyst preparation. It was pretreated by calcination in flowing O_2 at 400°C.

The supported catalysts were prepared as follows; each of the steps was carried out under dry N_2 (except when the catalyst precursor was $[H_2FeOs_3(CO)_{13}]$). Each cluster was dissolved in hexane at room temperature, and sufficient γ-Al_2O_3 was added to give the desired metal loading. The hexane was removed slowly from the slurry in a rotary evaporator, and the solid sample was dried under high vacuum for 1 h at room temperature.

Some preparations were carried out with a separate γ-Al_2O_3 support (Degussa Al_2O_3-C) to maximize the quality of the infrared spectra. Sufficient deionized water was added to the Al_2O_3 to make a paste. The material was dried in an oven at 120°C for 48 h and then calcined at 400°C in flowing O_2 for 4 h. Samples prepared from the Degussa Al_2O_3 were used only for infrared spectroscopy.

Catalytic Hydrogenation of CO

The catalysts were tested in a flow microreactor, described elsewhere (*6*), with Matheson UHP grade CO and H_2 as feed gases. In each experiment, 1–2 g of catalyst powder was loaded into the copper-lined tubular reactor between plugs of glass wool. The system pressure was brought to 10 atm with flowing H_2, and the catalyst was heated to 100°C. After 3 h, the flow of CO was started to give an equimolar H_2/CO feed stream. The total feed flow rate was set in the range 0.25 to 0.33 cm^3/s. After about 17 h, the temperature was increased to the desired reaction temperature (200 or 270°C) at a rate of 0.028°C/s.

The vapor-phase products flowed through a heated exit line to an on-line gas sampling valve for analysis with an Antek 300 gas chromatograph equipped with a flame ionization detector. Products were resolved in a 3.2-mm × 3.1-m column packed with particles of alumina.

Characterization of Catalysts

Elemental analysis. Some used catalyst samples were analyzed for Os by Schwarzkopf Microanalytical Laboratory, Woodside, N.Y. The Rh analyses were inconsistent and are not reported.

Electron microscopy. The used catalysts were examined with a Zeiss EM-10A transmission electron microscope. Samples were prepared (1) by embedding the catalyst in epoxy resin, microtoming a section, and then supporting it on a carbon-coated copper grid, or (2) by grinding the catalyst and dispersing it on a carbon-coated copper grid.

Infrared spectroscopy. Samples of catalyst were ground and pressed into wafers for characterization by infrared spectroscopy. The data were recorded with a Nicolet 7199 Fourier transform spectrometer; the sample cells and the vacuum/gas handling system are described elsewhere (*7*).

X-Ray photoelectron spectroscopy (XPS). XPS experiments were done with a Physical Electronics instrument (Model 550). Catalyst samples were used in the form of pressed wafers, unless otherwise noted, and handled in air prior to analysis.

TABLE 1

Compositions of Fresh Catalysts

Sample No.	Catalyst precursor	Metal loadings (wt%)[a]		
		Fe	Rh	Os
1	$[Rh_4(CO)_{12}]$	—	0.36	—
2	$[Rh_4(CO)_{12}]$	—	0.36	—
3	$[H_2RhOs_3(CO)_{10}(acac)]$	—	0.35	1.97
4	$[H_2RhOs_3(CO)_{10}(acac)]$	—	0.35	1.97
5	$[H_2FeOs_3(CO)_{13}]$	1.17	—	1.49

[a] Metal loadings determined from uptake of catalyst precursor.

RESULTS

The metal analyses of the catalysts are summarized in Table 1. The data for the fresh catalysts were determined from the cluster uptake from solution. Each of the catalysts containing Rh had an initial Rh content of about 0.35 wt%.

Each catalyst was found to be active for hydrogenation of CO, the products including both hydrocarbons and dimethyl ether (and, when yields of dimethyl ether were high, small amounts of methylethyl ether). The conversions were <3%, and products heavier than C_6 were not determined quantitatively. The conversion and product distribution data are presented in Table 2.

The catalytic activities and selectivities changed as a function of time on stream in the flow reactor. The most pronounced changes were in the yields of dimethyl ether, some of which increased markedly with increasing time on stream (Fig. 1). We infer that the ether was formed from dehydration of methanol (a primary product). The dehydration reaction is known to occur on the acidic γ-Al_2O_3 surface (*8*), and experiments with methanol as a feed to the flow reactor confirmed that it was dehydrated rapidly under conditions of the CO hydrogenation experiments.

Rates of CO conversion are summarized in Table 2. The rates were calculated from the initial metal loadings and the tabulated data on the basis of the assumption that conversions were differential. The rate of formation of each product can be calculated

TABLE 2

Catalyst Activities and Selectivities in CO Hydrogenation[a]

Catalyst sample No.	Catalyst precursor	Reaction temp. (°C)	Time on stream (h)	Conversion (%)	$10^4 \times$ rate (CO molecules/ metal atom · s)	Product composition (mol%)						
						CH_4	C_2	C_3	C_4	C_5	C_6	$(CH_3)_2O$
1	$[Rh_4(CO)_{12}]$	270	3	2.6	2.13	87.1	5.6	3.6	2.4	0.79	0.31	0.33
			5.5	2.4	1.97	87.4	5.4	3.4	2.4	0.80	0.33	0.40
			28.5	1.7	1.39	89.1	4.6	2.5	2.2	0.62	0.39	0.71
2	$[Rh_4(CO)_{12}]$	200	2.5	0.065	0.053	87.7	4.0	5.1	2.4	0.8	—	—
			7	0.089	0.073	83.0	4.5	6.2	3.1	1.7	0.9	0.7
			24	0.12	0.098	70.5	4.8	5.8	4.4	2.7	0.7	11.1
			31	0.12	0.098	69.4	4.6	5.3	3.8	2.1	0.7	14.0
			48	0.11	0.090	67.7	4.3	4.9	3.8	2.3	0.8	16.4
3	$[H_2RhOs_3(CO)_{10}(acac)]^b$	270	3.5	1.5	0.26	68.8	8.9	10.1	5.8	2.6	1.4	1.5
			7	1.4	0.25	69.1	8.6	9.8	5.7	2.4	2.0	2.4
			24	1.0	0.18	72.1	8.3	9.0	5.4	2.4	1.3	1.5
4	$[H_2RhOs_3(CO)_{10}(acac)]^c$	200	2	0.099	0.026	62.1	8.3	22.7	4.9	2.0	—	—
			4	0.079	0.021	73.8	7.0	13.4	4.2	1.5	—	—
			6	0.073	0.019	75.7	7.5	11.3	3.4	1.1	—	1.0
			30	0.078	0.020	67.2	4.9	7.0	4.1	2.1	—	14.8
			72	0.070	0.018	67.7	3.7	6.2	4.8	2.5	0.7	14.5
5	$[H_2FeOs_3(CO)_{13}]$	270	11	0.033	0.0033	67.4	17.9	5.0	3.2	1.9	0.5	4.2
			24	0.032	0.0032	62.7	15.9	1.6	1.6	1.3	0.6	16.4
			55	0.036	0.0036	49.0	11.2	1.0	0.8	1.0	0.7	36.4

[a] Reactor pressure = 10 atm.
[b] The Os content measured after 24 h on stream was 0.90%.
[c] The Os content measured after 72 h on stream was 0.36%.

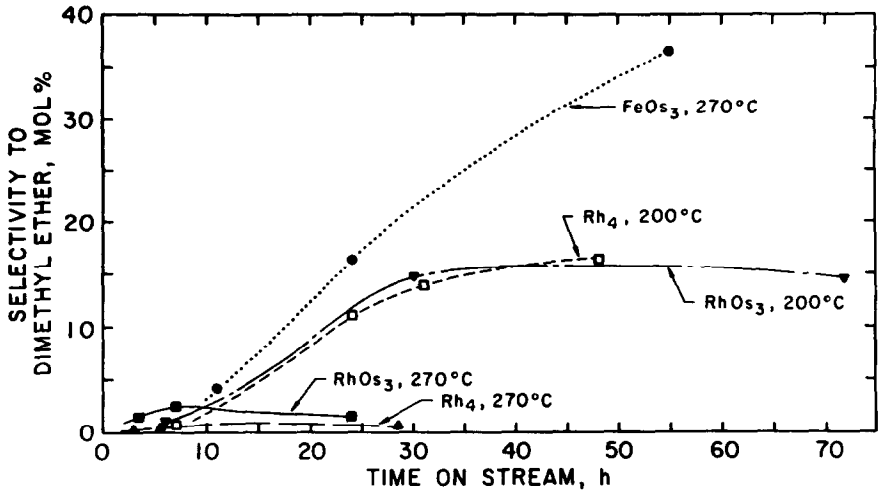

FIG. 1. Development of selectivity for formation of dimethyl ether from an equimolar mixture of CO and H_2 at 10 atm. The catalysts are specified in Table 1.

from the tabulated rates and the product distributions (Table 2).

The major product observed in each experiment was methane. The hydrocarbon products were formed in approximately a Schulz–Flory–Anderson distribution; typical data are shown in Fig. 2. There was no marked selectivity to olefin.

The selectivities to oxygenated product were favored by low temperature and by the presence of Os with Rh in the catalyst; the $FeOs_3$ catalyst had an especially high selectivity for ether formation but a low overall activity. The $RhOs_3$ catalyst was less active than the Rh catalyst—even with the rates for each catalyst represented per Rh atom.

Electron micrographs of the catalysts used at 270°C (e.g., Fig. 3) showed that small particles were present on the γ-Al_2O_3 support. The typical particle size range was 15–30 Å for the $RhOs_3$ catalyst (sample 3) and 20–30 Å for the $FeOs_3$ catalyst (sample 5). No larger supported metal particles were visible in these samples. In the catalysts used at the lower temperature (200°C) (samples 2 and 4), no supported particles were visible.

The XPS results indicated the presence of zero-valent Rh in the Rh-containing catalysts. The used catalyst prepared from [$Rh_4(CO)_{12}$] (sample 1) and that prepared from [$H_2RhOs_3(CO)_{10}$(acac)] (sample 3) had Rh $3d_{5/2}$ peaks at 307 eV; Rh foil was found to have a peak at this same position.

The used catalyst prepared from [$H_2RhOs_3(CO)_{10}$(acac)] (sample 3) had Os $4f_{7/2}$ and Os $4f_{5/2}$ peaks at 51.5 and 53.3 eV, respectively. Knözinger *et al.* (*9*) reported an Os $4f_{7/2}$ peak at 52.3 eV for a γ-Al_2O_3-sup-

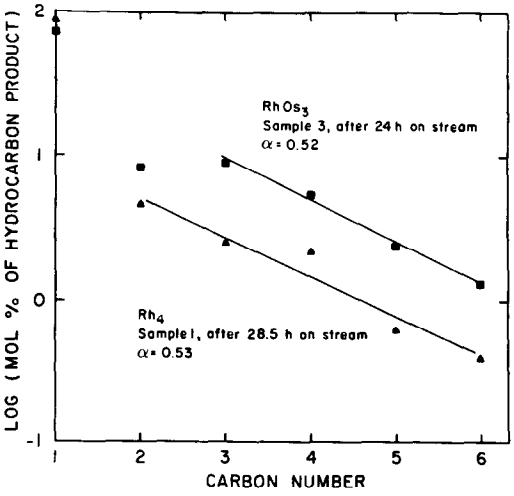

FIG. 2. Distributions of hydrocarbon products formed from CO and H_2 at 270°C. The catalysts are specified in Table 1.

FIG. 3. Electron micrograph of used catalyst derived from $[H_2RhOs_3(CO)_{10}(acac)]$ (sample 3). The sample used for the electron microscopy was prepared by method (2), described in the text.

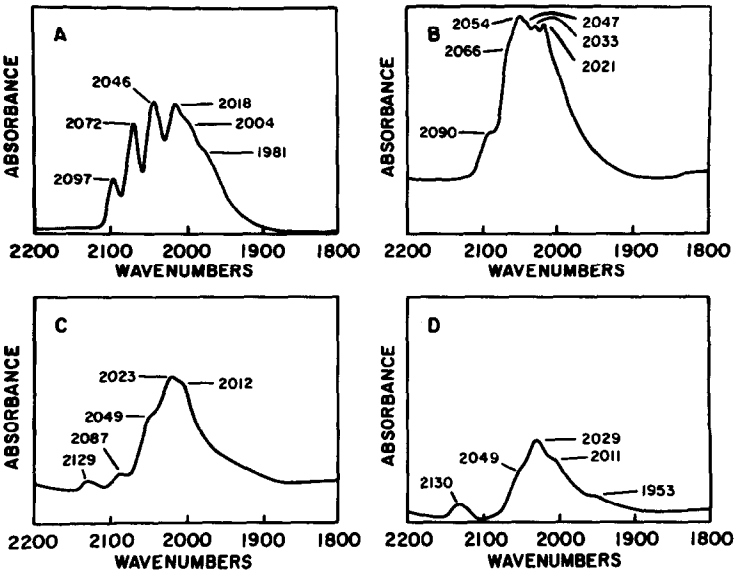

FIG. 4. Infrared spectra of $[H_2RhOs_3(CO)_{10}(acac)]$ on γ-Al_2O_3: (A) the initially adsorbed material; (B) after heating at 100°C in equimolar H_2 + CO; (C) after heating at 200°C for 1.25 h in equimolar H_2 + CO; and (D) after heating at 270°C for 1 h.

ported sample prepared from $[Os_3(CO)_{12}]$; the high binding energy implies that Os was present in an oxidized state.

Only imprecise XPS data were obtained with the used catalyst prepared from the Fe Os_3 cluster; the data were obtained with powder on adhesive tape, rather than with a pressed wafer. The Fe $2p_{3/2}$ peak was observed as a weak, broad band centered at 710 eV; this binding energy is characteristic of Fe_2O_3 and suggests that Fe was present in a mixture of different oxidation states.

The analyses of the used catalysts (Table 2) showed that Os was lost during operation. The decreases in Os contents indicate that Os was mobile, possibly being present as volatile carbonyls which moved downstream and out of the catalyst bed.

Infrared spectra of the catalysts were recorded at various stages of preparation. Typical results are shown in Fig. 4 for a sample prepared from $[H_2RhOs_3(CO)_{10}(acac)]$ and Al_2O_3. These spectra are indicative of changes in the surface organometallics during heating in an equimolar mixture of flowing H_2 + CO; they are therefore representative of the catalyst break-in period—except that the support was Degussa Al_2O_3 (rather than Catapal) and the pressure was 1 atm (rather than 10 atm). Similar experiments were done with samples prepared from $[H_2FeOs_3(CO)_{13}]$ and the Degussa Al_2O_3; results are shown in Fig. 5.

The used catalysts were also characterized by infrared spectroscopy in the carbonyl region; results are presented in Table 3. Carbonyl bands were observed for all the used catalysts except those prepared from the tetrarhodium cluster.

DISCUSSION

$RhOs_3$ Catalysts

Comparison of the infrared spectra of the organometallic species initially prepared from $[H_2RhOs_3(CO)_{10}(acac)]$ on the γ-Al_2O_3 support (Fig. 4A) with the nearly identical spectrum of the molecular cluster itself (Table 3) leads to the conclusion that the cluster initially was physically adsorbed on the Al_2O_3. The spectra of Fig. 4B–D show the changes which occurred upon heating of

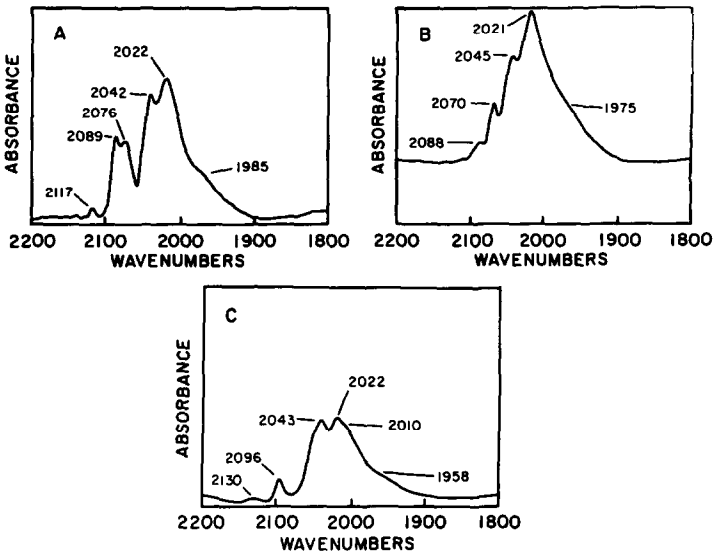

FIG. 5. Infrared spectra of $[H_2FeOs_3(CO)_{13}]$ on γ-Al_2O_3: (A) the initially adsorbed material; (B) after heating at 100°C in equimolar H_2 + CO for 1 h; and (C) after heating at 225°C in equimolar H_2 + CO for 1 h.

the sample under an atmosphere of CO + H_2 up to the higher catalyst operating temperature (270°C). The chemistry involved here may be interpreted on the basis of well-established solution and surface chemistry, as follows:

Farrugia *et al.* (*4*) reported that $[H_2RhOs_3(CO)_{10}(acac)]$ reacts very rapidly with CO, as follows:

$$[H_2RhOs_3(CO)_{10}(acac)] + 3CO \rightarrow [Rh(acac)(CO)_2] + [Os_3H(\mu\text{—}H)(CO)_{11}] \quad (1)$$

We have confirmed that this cluster breakup occurs readily in hexane solution. Therefore, we suggest that the surface chemistries of $[Rh(acac)(CO)_2]$ and $[Os_3H(\mu\text{—}H)(CO)_{11}]$ should be considered in attempts to interpret the data of Fig. 4.

After heating of $[H_2RhOs_3(CO)_{10}(acac)]$/$\gamma$-$Al_2O_3$ to 100°C under H_2 + CO, spectrum B of Fig. 4 was obtained. The bands at 2066, 2054, and 2021 cm^{-1} agree closely with those of the relatively well-characterized surface-bound cluster $[Os_3(\mu\text{—}H)(CO)_{10}(O\text{—}Al<)]$ (*10–12*), which can be formed by an oxidative addition reaction involving $[Os_3(CO)_{12}]$ and surface hydroxyl groups (*10, 12*) or by a similar reaction involving $[Os_3(\mu\text{—}H)_2(CO)_{10}]$ and surface hydroxyl groups (*10*). The carbonyl peaks located at 2090 and 2033 cm^{-1} are tentatively assigned to a $Rh^I(CO)_2$ complex (*13, 14*). The interpretation of these results is similar to that of Choplin *et al.* (*15*), who investigated the reaction of $[H_2FeOs_3(CO)_{13}]$ on SiO_2 to give $Os_3(\mu\text{—}H)_2(CO)_{10}(O\text{—}Si<)$.

Heating the sample to a higher temperature (200°C) under H_2 + CO resulted in a new spectrum (2129w, 2087w, 2049sh, 2023s, 2012s; Fig. 5, Spectrum C), which is closely similar to that reported for the cluster anion $[H_3Os_4(CO)_{12}]^-$ [2119w, 2083w, 2048s, 2022s, 2000s, 1976w] (*16*). The reaction forming the tetranuclear cluster is suggested to be analogous to the reaction of $[Os_3(CO)_{12}]$ with H_2 in refluxing octane to give $[H_4Os_4(CO)_{12}]$ (*17*); this neutral cluster reacts with the Al_2O_3 surface to give the cluster anion (*18*), the chemistry being closely similar to that observed for $RuOs_3$ clusters at low temperatures (*19, 20*). The bands assigned to $Rh^I(CO)_2$ in the sample

TABLE 3

Infrared Spectra of Molecular and Supported Organometallics

Sample or precursor	Solvent or support	ν(CO) (cm^{-1})	Ref.
Molecular metal clusters			
$[H_2RhOs_3(CO)_{10}(acac)]$	Cyclohexane	2096w, 2071s, 2049s, 2010s, 2002m(sh), 1990m, 1983m, 1976m	This work
$[H_2FeOs_3(CO)_{13}]$	Hexanes	2086s, 2072s, 2040s, 2032m, 2025m, 2015w, 1994w, 1877vw, 1847w	This work
Supported complexes and clusters			
$[HOs_3(CO)_{10}—O—Al\lessdot]$	γ-Al_2O_3	2107w, 2068s, 2056s, 2023vs, 2005m	(*12*)
$[Os(CO)_x(O—Al\lessdot)_2]$, x = 2 or 3	γ-Al_2O_3	2130m, 2030–2050s, 1940–1970m	(*11–13*)
$Al^+[H_3RuOs_3(CO)_{12}]^-$	γ-Al_2O_3	2051s, 2020s, 2010s, 1975sh	(*20*)
Supported organometallics derived from clusters			
$[H_2RhOs_3(CO)_{10}(acac)]^a$	γ-Al_2O_3	2096m, 2072s, 2046s, 2018s, 2004m(sh), 1981m(sh)	This work
$[H_2RhOs_3(CO)_{10}(acac)]^{a,b}$	γ-Al_2O_3	2090w, 2066s(sh), 2054s, 2047sh, 2033sh, 2021s	This work
$[H_2RhOs_3(CO)_{10}(acac)]^{a,c}$	γ-Al_2O_3	2129w, 2087w, 2049sh, 2023s, 2012s	This work
$[H_2RhOs_3(CO)_{10}(acac)]^{a,d}$	γ-Al_2O_3	2130m, 2049sh, 2029s, 2011sh, 1953sh	This work
$[H_2FeOs_3(CO)_{10}]^a$	γ-Al_2O_3	2117w, 2089m, 2076m, 2042s, 2022s, 1985m(sh)	This work
$[H_2FeOs_3(CO)_{10}]^{a,b}$	γ-Al_2O_3	2088vw, 2070w, 2045m, 2021s, 1975m(sh)	This work
$[H_2FeOs_3(CO)_{10}]^{a,e}$	γ-Al_2O_3	2130vw, 2096w, 2043s, 2022s, 2010s, 1958w(sh)	This work
$[HOs_3(CO)_{10}—(O—Al\lessdot)]^e$	γ-Al_2O_3	2121w, 2095w, 2045s, 2021s, 2007sh	This work
Used catalysts			
Sample 1	—	No carbonyl bands	This work
Sample 2	—	No carbonyl bands	This work
Sample 3	—	2123m, 2033s, 1949m	This work
Sample 4	—	2124w, 2048s, 2025s, 2003m, ~1950sh	This work
Sample 5	—	2124m, 2033s, 1943m	This work

[a] Precursor.
[b] After reaction in equimolar H_2 + CO at 100°C.
[c] After reaction in equimolar H_2 + CO at 200°C.
[d] After reaction in equimolar H_2 + CO at 270°C.
[e] After reaction in equimolar H_2 + CO at 225°C.

heated to 200°C are greatly diminished in intensity.

After treatment of the sample in H_2 + CO at a still higher temperature, 270°C, significant cluster break-up was apparent (Fig. 4, Spectrum D), as shown by the bands at 2130, 2029, and 1953 cm^{-1}, which are indicative of the mononuclear Os(II) carbonyl

complex, $Os(CO)_x(O—Al<)_2$, where $x = 2$ or 3, which has been observed to result from decomposition of oxide-supported triosmium clusters (*10–12*). No $Rh^I(CO)_2$ bands were evident, and we infer from the microscopy and XPS data that particles of metallic Rh had formed. The infrared spectrum of CO adsorbed on alumina-supported Rh particles shows bands at 2035(s) and 1825(wbr) cm^{-1} (*14*). Unfortunately, the 2035-cm^{-1} peak overlaps the osmium carbonyl bands, making it impossible to detect.

The characterization of the used Rh-containing catalysts by XPS demonstrated that zero-valent Rh was present, but there was no XPS evidence for zero-valent Os; we therefore infer that the small particles observed by electron microscopy were almost entirely Rh. The infrared spectra of the used $RhOs_3$ catalysts are consistent with this interpretation, demonstrating the presence of mononuclear Os complexes.

In summary, then, the physical characterization data lead to the conclusion that the $RhOs_3$ clusters broke up and formed segregated metal species in the catalyst. The catalyst performance data support this conclusion, as follows: (1) the activities per Rh atom of the catalysts prepared from $[Rh_4(CO)_{12}]$ and $[H_2RhOs_3(CO)_{10}(acac)]$ are roughly the same (Table 2); (2) the rates of deactivation (Table 2) and the development of oxygenate selectivity (Fig. 1) are approximately the same for these two catalysts, and (3) their Schulz–Flory–Anderson plots (Fig. 2) are similar [the values of the chain growth probability (α) being about 0.5 for each catalyst (after 24–28.5 h on stream)].[4]

We conclude, therefore, that virtually all the catalytic activity of the $RhOs_3$ catalyst is to be attributed to the Rh. The Os, at most, appears to increase slightly the selectivity for oxygenate formation (Fig. 1).

Selectivity for oxygenate formation in the presence of highly dispersed Rh catalysts on Al_2O_3 supports has been observed before (*2*); much higher oxygenate selectivities have been observed with Rh on basic oxide supports (*2*). The cause of this selectivity is still debated, but some authors attribute it to the presence of ionic species, e.g., Rh ions in rhodium oxides (*21*).

The oxygenate selectivity increased markedly with time on stream in experiments with the Rh-containing catalysts at 200°C. In contrast, the same catalysts at 270°C gave only minimal ether yields. It is possible that the primary oxygenated product (methanol) was formed at Rh(I) sites which were stabilized by the alumina support at 200°C (but not at 270°C). The *in situ* infrared experiments with $[H_2RhOs_3(CO)_{10}(acac)]$ on γ-Al_2O_3 provide some support for this hypothesis. After heating of the sample to 200°C under H_2 + CO, evidence for surface Rh(I) carbonyl complexes was obtained, but with a similar treatment at 270°C, no such species were detected.

Alternatively, the higher oxygenate yield at 200°C could be explained by the suggestion that the ability of the Rh metal to adsorb CO dissociatively is significantly less at 200°C than at 270°C. It is known that higher reaction temperatures favor CO dissociation and the corresponding production of hydrocarbons; conversely, there is a correlation between the selectivity of a metal catalyst for methanol formation and nondissociative adsorption of CO (*22*).

The Rh-containing catalysts were an order of magnitude more active at 270°C than at 200°C and underwent deactivation at higher rates at the higher temperature. The catalyst deactivation was probably a result of carbonaceous deposits, although there may have been some initial activity loss at 270°C resulting from aggregation of Rh metal and loss of surface area. Electron microscopy indicated that 15- to 30-Å parti-

[4] The catalysts prepared from $[H_2RhOs_3(CO)_{10}(acac)]$ gave abnormally high C_3 product yields in the initial period of each test. This result is attributed to the decomposition of the acac ligand originally present in the catalyst precursor. Interestingly, the initial C_2 yields were not high, which suggests that this fragment of the acac ligand was readily incorporated in the hydrocarbon chain-growth products.

cles were formed on catalysts tested at 270°C. However, no surface aggregates were detected with catalysts used at 200°C, which suggests that the metal particles were very small.

$FeOs_3$ Catalysts

The infrared experiments carried out with $[H_2FeOs_3(CO)_{13}]$ adsorbed on γ-Al_2O_3 indicate that the surface chemistry is similar to that of $[H_2RuOs_3(CO)_{13}]$ on γ-Al_2O_3 (*19, 20*). The initially adsorbed species exhibited bands at 2089, 2076, and 2042 cm^{-1} (Fig. 5, Table 3), which are indicative of unreacted $[H_2FeOs_3(CO)_{13}]$. We suggest that the original cluster was present in a mixture with other $FeOs_3$ carbonyls—possibly including $[HFeOs_3(CO)_{13}]^-$. Heating the sample to 225°C in H_2 + CO led to changes in the spectrum which are suggestive of the formation of the cluster anion $[H_3FeOs_3(CO)_{12}]^-$ (Fig. 5, Spectrum C; Table 3). [Compare the spectrum of this sample (2130vw, 2096w, 2043s, 2022s, 2010s, 1958sh cm^{-1} with that of $[H_3RuOs_3(CO)_{12}]^-$ in CH_2Cl_2 solution (*19*) (2044s, 2040sh, 2020s, 1999s, 1976m, 1946w, 1918w cm^{-1}).] The carbonyl peak intensities of the surface species were reduced in this sample, suggesting that some metal carbonyls had been volatilized. When the sample was heated to 270°C, cluster decomposition evidently occurred to give $Os(CO)_x(O—Al\lessdot)_2$ (x = 2 or 3) and iron species.

The catalysts derived from $[H_2FeOs_3(CO)_{13}]$ supported on γ-Al_2O_3 were found to be two orders of magnitude less active than the Rh-containing catalysts at 270°C. There was a significant evolution in performance of the $FeOs_3$ catalyst during the experiment, characterized by increasing oxygenate selectivity and declining hydrocarbon production, with the overall activity remaining approximately constant (Fig. 1 and Table 2). The XPS and infrared data characterizing the used $FeOs_3$ catalysts suggest that oxidized Fe and $Os(CO)_x(O—Al\lessdot)_2$ species were present. The 20- to 30-Å particles observed in the electron micrographs of the catalyst are suggested to be indicative of an oxidized iron phase.

The performance of the $FeOs_3$ catalyst was quite different from that observed with catalysts derived from $[Fe_3(CO)_{12}]$ deposited on γ-Al_2O_3 (*23*), which showed high selectivity for light olefins. The latter catalysts had higher iron loadings than used here (0.5–0.8 wt%), and metallic iron particles were formed upon decomposition of the $[Fe_3(CO)_{12}]$ (*23*). The different behavior of $[H_2FeOs_3(CO)_{12}]/\gamma$-$Al_2O_3$ may be attributed to its lower Fe loading and also the stability of the intermediate surface cluster $Al^+[H_3FeOs_3(CO)_{12}]^-$. This cluster was shown to decompose at temperatures >225°C, at which reaction of the iron carbonyl fragment with surface hydroxyl groups is known to occur to give oxidized iron species and H_2 (*24*). The oxidized surface iron species, once formed, are known to be highly resistant to reduction to the metallic state under the synthesis conditions employed (*24, 25*).

ACKNOWLEDGMENTS

We thank J. H. Onuferko for the XPS measurements. B. F. Lücke was supported through an agreement between the Akademie der Wissenschaften der DDR and the U.S. National Academy of Sciences. The work was supported by the National Science Foundation.

REFERENCES

1. Sinfelt, J. H., "Bimetallic Catalysts, Discoveries, Concepts, and Applications." Wiley, New York, 1983.
2. Katzer, J. R., Sleight, A. W., Gajardo, P., Michel, J. B., Gleason, E. F., and McMillan, S., *Faraday Discuss. Chem. Soc.* **72,** 121 (1981), and references cited therein.
3. Budge, J. R., Lücke, B. F., Scott, J. P., and Gates, B. C., in *Proc. Int. Congr. Catal. 8th* **5,** 89 (1984).
4. Farrugia, L. J., Howard, J. A. K., Mitrprachachon, P., Stone, F. G. A., and Woodward, P., *J. Chem. Soc. Dalton* 171 (1981).
5. Burkhardt, E. W., and Geoffroy, G. L., *J. Organometal. Chem.* **198,** 179 (1980).
6. Baek, K. H., Ph.D. thesis, University of Delaware, Newark, in preparation.
7. Barth, R., Gates, B. C., Zhao, Y., Knözinger, H., and Hulse, J., *J. Catal.* **82,** 147 (1983).

8. Knözinger, H., *Angew. Chem. Int. Ed. Engl.* **7,** 791 (1968).
9. Knözinger, H., Zhao, Y., Tesche, B., Barth, R., Epstein, R., Gates, B. C., and Scott, J. P., *Faraday Discuss. Chem. Soc.* **72,** 53 (1981).
10. Psaro, R., Ugo, R., Zanderighi, G. M., Besson, B., Smith, A. K., and Basset, J. M., *J. Organometal. Chem.* **213,** 215 (1981).
11. Deeba, M., and Gates, B. C., *J. Catal.* **67,** 303 (1981).
12. Knözinger, H., and Zhao, Y., *J. Catal.* **71,** 337 (1981).
13. Foley, H. C., DeCanio, S. J., Tau, K. D., Chao, K. J., Onuferko, J. H., Dybowski, C., and Gates, B. C., *J. Amer. Chem. Soc.* **105,** 3074 (1983), and references cited therein.
14. Theolier, A., Smith, A. K., Leconte, M., Basset, J. M., Zanderighi, G. M., Psaro, R., and Ugo, R., *J. Organometal. Chem.* **191,** 415 (1980).
15. Choplin, A., Leconte, M., Basset, J. M., Shore, S. G., and Hsu, W.-L., *J. Mol. Catal.* **21,** 389 (1983).
16. Johnson, B. F. G., Lewis, J., Raithby, P. R., Sheldrick, G. M., Wong, K., and McPartlin, M., *J. Chem. Soc. Dalton,* 673 (1978).
17. Knox, S. A. R., Koepke, J. W., Andrews, M. A., and Kaesz, H. D., *J. Amer. Chem. Soc.* **97,** 3942 (1975).
18. Krause, T., Davies, M. E., Lieto, J., and Gates, B. C., to be published.
19. Budge, J. R., Scott, J. P., and Gates, B. C., *J. Chem. Soc. Chem. Commun.,* 342 (1983).
20. Scott, J. P., Budge, J. R., Rheingold, A., and Gates, B. C., to be published.
21. Watson, P. R., and Somorjai, G. A., *J. Catal.* **72,** 347 (1981).
22. Klier, K., *in* "Catalysis of Organic Reactions" (W. R. Moser, Ed.), p. 195. Dekker, New York, 1981.
23. Commereuc, D., Chauvin, Y., Hugues, F., Basset, J. M., and Olivier, D., *J. Chem. Soc. Chem. Commun.,* 154 (1980).
24. Brenner, A., and Hucul, D. A., *Inorg. Chem.* **18,** 2836 (1979).
25. Blanchard, F., Raymond, J. P., Pommier, B., and Teichner, S. J., *J. Mol. Catal.* **17,** 171 (1982).